

Crustal and upper mantle structure in eastern boundary of Tibet plateau by MT data

ZHAO Guoze, CHEN Xiaobin, TANG Ji, SUN Jie, WANG Lifeng, WAN Zhansheng, ZHAN Yan
Institute of Geology, China Earthquake Administration, Beijing, China

SUMMARY

Eastern boundary area of Tibet plateau is one of the significantly deformed and the most earthquake-active regions in china continent. There are many seismically active faults. MT data were obtained along a profile SMp of 145km long that started from Chuan-Dian (Sichuan province-Yunnan province) block (CDB), crossing Da-Xue-Shan block (DXSb) and ended in Central Sichuan block (CSb) with striking in NEE direction. The remote reference MT method and robust technique were used in the field measurement and data processing. The impedance tensor decomposition was carried out for study of local distortion of the data. The static correction factors was calculated for static shift data. 2-D electrical structure along profile was obtained by using topographic 2-D inversion method NLCCG.

The 2-D electrical structure can be divide into three segments, CDB block, DXSb block and CSb block. In CDB block and DXSb block, a high resistivity layer of eastward thrusting with “axe” shape appeared in the upper crust, the low resistivity layer with eastward subducting in the middle crust and a relative higher resistivity in the lower crust and upper mantle. The joined faults XA faults of Xian-Shui-He faults with An-Ning-He faults, a significantly active fault belt, is a lithospheric faults and cut off by low resistivity layer in the middle crust. The frequent occurrence of micro-seismicity appeared in the joint area. The geometric and kinematic characteristics of the crust is postulated to be relative to three actions: eastward force of Tibet, clockwise movement of the CDB and DXSb blocks and resisting of the CSb.

Keywords: Magnetotellurics, electrical structure, active faults, Tibet plateau

INTRODUCTION

The east boundary area of Tibet plateau is one of significantly deformed and mostly active earthquake regions either in china continent or in the world. There developed many active faults in study area. There occurred 48 earthquakes of magnitude 6~6.9 and 18 earthquakes of 7~7.9 in study area and the surrounding since 16 B.C. (Xu, X. et al, 2005). Five strong shocks of magnitude of 7~7.9 occurred only along XSH faults (about 400km long) crossing this MT profile during last century (Wen, X., et al, 2003).

Since 70's of last century this area has been drawing a lot of geologists to study the fault

distribution, faulting segmentation, seismic activity and geodynamics etc (Deng, Q., et al, 1994). But only a few geophysical measurements have been carried out because severe topography in this area (Sun, J. et al, 2003, Wang, C. 2003). In this paper we will present the newest results on 2-D electrical structure of the crust and upper mantle along a profile and its tectonic meaning. The study purpose is on the characteristics of active faults, fault manner at depth and to provide the data for research of risk of recurrence of strong earthquakes.

GEOLOGIC SETTING

Recently we have measured the magnetotelluric data along a profile from Shi-Mian city (SMc) to Le-Shan city (LSc) in eastern boundary area of Tibet plateau (profile SLp in Fig.1). The profile started from rhombus Chuan-Dian block (CDB), crossing Da-Xue-Shan block (DXSb) and ended in Central Sichuan block (CSb) with striking about N80°E. The profile was 145 km long. The CDB is a internal subblock of Tibet plateau and CSb is a subblock of stable south china block. DXSb is in between them (Fig. 1).

Under the united east-southward actions by Tibet plateau and other blocks, rhombus CDB appears to move clockwise with southward. As the northeastern and eastern boundary faults of CDB, XA changed its movement from extension in the early Pleistocene to the left lateral slip in the later Pleistocene (Shen, Z., et al, 2005). MT profile crossed many active faults. In order to present faults easier, we list their names and positions in distance relative to west end (0 km) of profile respectively. XA faults is consisted of famous active Xian-Shui-He (XSH) faults north of the profile and An-Ning-He (ANH) faults south of the profile. MT profile crossed joint point of XSH and ANH at about 10km. Wan-Yuan faults (WY) is at about 27 km, Han-Yuan faults (HY) at 55km, Feng-Yi faults (FY) at 65km, Da-Xiang-Ling (DXL) at 80km, Liujiang-Hongxi (LH) at 95km, E-Bian faults (EB) at 105km and Ma-Bian faults (MB) at 135km (Fig.1). XA faults is considered a part of the longer lithospheric faults (Wang, Z., et al, 1996). ANH is the boundary faults between CDB and DXSb (Ma, X. 1989). The crust thickness along the profile is charactered by transition zone. The depth of Moho is about 56 km at west end and 43 km at east end (Bureau of Geo. and Mine. of Sichuan Province, 1982). The horizontal velocity by GPS data between 1998

and 2004 indicated that left slip across XSH is 10~11 mm/yr and left slip across ANH is ~7mm/yr (Shen, Z., et al, 2005).

Most notably, quite frequent occurrence of the earthquakes existed along the XA faults and other faults, but the magnitude of the earthquake and the epicenter distribution were closely relative to the different segments of the faults (Tang, R., et al, 1992, Wang, X., et al, 1998,).

MAGNETOTELLURIC DATA

Magnetotelluric data are obtained at 77 sites along the profile SLp with smallest site span of about a few hundreds meters. The remote reference MT method (RRMT) was used in the field measurement and robust technique in the data processing (Zhao, G. 1986a, Zhang, Q., et al, 2002). Due to the limitation by severe topography some sites were located near electric power stations and rather bigger noise appeared in apparent resistivity and phase at some of sites even though RRMT and robust were used. Except for the noisy sites, available MT data at 68 sites can be used in the interpretation. The impedance tensor decomposition (Bahr, K., 1988, Zhao, G., et al, 1996b) was made and it was found that local distortion for most sites are weak and skewness are less than 0.3~0.4 for most data along profile. The static correction factors were calculated and used in apparent resistivity for static shifted data. The pseudosections of apparent resistivity and impedance phase are shown in the top picture in Fig. 3.

2-D ELECTRICAL STRUCTURE

The MT data along the profile were inverted by using topographic 2-D inversion method NLGG

(Rodi W, Mackie R L. 2001). In the calculation the grids of the model was designed to match the topographic elevation as better as possible. Fig.2 shows the topography and the grids of the model on the surface. In case of the different site spans in different sections of the profile and of the severe topography along the profile, we firstly divided the profile into 4 sections and inversed the data respectively for them. When data fittings was satisfied for each section 2-D inversion was carried out for data in whole profile where the initial model was selected by combination of final models of 4 sections. We also tried to respectively use different polarization of the data, TM, TE, both TM and TE in the 2-D inversion. The results indicated that the best fitting of the data came from modeling by TM polarization data. Thus 2-D electrical structure of the crust and upper mantle was obtained by using TM data. The pseudosections of observed data and model data for TM apparent resistivity and phase are shown in Fig.3. The fitting error for either apparent resistivity or phase are less than 10% for most data but it is the better for apparent resistivity than phase. The final 2-D model is shown in Fig.4.

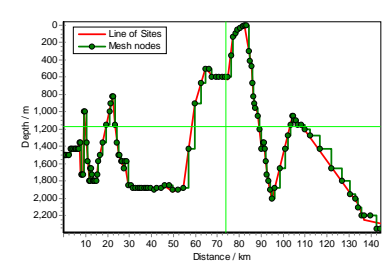


Fig.2 Topography and model grids on the surface of earth along profile

A clear electrical boundary appears in the position of 95km corresponding to the EB faults in between DXSb and CSb. There is a significant

difference of the resistivity structure between its both sides.

The layering structure appears west of EB faults. A high resistivity layer with resistivity of a few hundreds to a few thousands Ohm-meters occurs in the upper crust from 0 km to YJ faults (80km). The thickness of high resistivity layer decreases gradually from about 20 km thick at west end (0km) to zero at YJ faults. The high resistivity layer with “axe” shape is cut off by a few fault belts producing several segments in profile. These fault belts have different inclination and width. The XA fault belt and WY fault belt with about a few km width respectively have steep inclination angle. The lower resistivity appears inside XA and WY fault belts. HY, DXL and LH fault belts incline to the west and are postulated to be thrust faults.

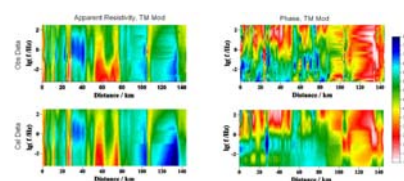


Fig. 3 The comparison of observed data (on the top) and theoretical data by 2-D modelling (on the bottom). The left is pseudosections of apparent resistivity and the right is phase

A low resistivity layer appears below the upper crustal high resistivity layer. Its resistivity and thickness varies in lateral direction. The resistivity is ranging from tens to more than hundred Ohm-meters. The thickest part of about 20 km appears at west end of the profile and then gradually reduces eastward along profile. The smallest thickness of about 10 km appears at 55km beneath HY faults.

The shape and thickness of low resistivity layer in the middle crust changes greatly in the

segment east of point 55km in profile where the layer starts eastward subducting and the thickness changes to about 30~40 km thick. The combination of the high resistivity layer in upper crust with low resistivity layer in middle crust forms a “pincelike” structure.

Under the low resistivity layer in middle crust the resistivity increases in the lower crust and upper mantle. Within this region the resistivity is larger in between XA faults and FY faults than in its both sides.

The resistivity in the upper and middle crust in segment east of EB faults is high in general without low resistivity layer. Below that the resistivity decreases with depth. Therefore the boundary corresponding to the EB faults is postulated to be a significant fault belt separating DXSb subblock and CSb subblock.

2-D electrical structure also shown that the XA fault belt is divided into two parts vertically. The top part in the upper crust has low resistivity. The bottom part in lower crust and the below is a electrical boundary with lower resistivity west of it and higher resistivity east of it. In the middle crust XA fault belt is cut off by low resistivity layer.

The geologic data indicated that ductile-shear zone existed along XA faults and mylonite developed there (Wang, Z., et al, 1996). Thus the low resistivity layer in the middle crust west of EB faults is possibly a crustal detachment layer. Therefore it may interpret why the great frequent occurrence of small earthquakes appeared in the connection area of XA faults (joint place of XSH faults and ANH faults) and the many stronger earthquakes appeared in other segments of XSH faults and ANH faults.

CONCLUSION AND DISCUSSION

The electrical structure along MT profile can be divide into three segments corresponding to CDb, DXSb and CSb respectively. The similar layering crustal structure appears for CDb and DXSb which is great different from that of CSb. Three segments are separated by lithospheric faults, XA fault belt and EB fault belt respectively. The XA fault belt is discontinuous in middle crust that is possibly due to the detachment movement in middle crust that cuts off XA fault belt laterally.

The foci of earthquake were generally at depth less than about 20km (Tang, et al, 1992) that was just corresponding to the high resistivity layer in the upper crust.

The “pincelike” electrical structure of the crust west of EB can be compared to that of a parallel profile north of this profile (Sun, J.,et al, 2003). The later crossed XSH faults and Longmenshan faults.

The induction arrows in frequency band from 1 Hz to several hundreds Hz also indicates that the low resistivity layer exists in the middle crust agreeable to 2-D model and is more conductive in the region south of this profile.

The crustal structure along the MT profile is formed owing to three actions: southeastward movement of Tibet plateau, clockwise movement of the CDb and resisting force of stable CSb. But the detailed dynamic process and its relationship with seismic activity are still unclear and need further investigation.

REFERENCE

- Bahr K., 1988. Interpretation of the magnetotelluric impedance tensor: regional induction and local telluric distortion J Geophysics,62: 119-127
- Bureau of Geo. and Mine. Sichuan Province, Regional Geology of Sichuan province, Geological Publishing House , Beijing, 1982
- Deng, Q., Chen, S., Zhao, X., 1994, Tectonics, seismicity and dynamics of Longmenshan Mountains and its adjacent regions[J]. Seismology and Geology, 16(4): 389-403
- Ma, X.,(ed), Lithospheric Dynamics Atlas of China[z] . China Cartographic Publishing House, Beijing, 1989
- Rodi W, Mackie R L. 2001, Nonlinear conjugate gradients algorithm for 2-D magnetotelluric inversion. Geophysics, 66(1):174-187
- Shen, Z., Lu", J., Wang, M., Bu" rgmann, R., 2005, Contemporary crustal deformation around the southeast borderland of the Tibetan Plateau, J.G.R., VOL. 110, B11409
- Sun, J., et al, 2003. Sounding of electrical structure of the crust and upper mantle along the Zhang, Q., Yang,S., 2002,An application study of noise elimination for magnetotelluric sounding data, Geophysical Prospecting for Petroleum, Vo1. 41,No.4, 493-499
- Zhao, G., 1986a, Magnetotelluric investigation of the earth crust and upper mantle and the referencr channel method, in "Collected Works Zhao, G., Tang, J., Liu, T., et al, 1996b, Preliminary interpretation of MT data along eastern border of Qinghai-Tibet Plateau and its tectonic significance[J]. Science in China(Ser D), 46 (Supp1): 243-253
- Tang, R., Qian,H., Huang, Z., et al, 1992, The Feature of Activity on the Noah Segment of the Anninghe Fracture Zone since Late Pleistocene, Earthquake Research in China, VO1. 8. NO. 3, 60-68
- Wang, C., Wu, J., Lou., H., et al, 2003. P-wave crustal velocity structure in western Sichuan and eastern Tibetan region[J]. Science in China(Ser D), 46(Supp1): 254-265
- Wang, X., Zhang C., Pei X., 1998, Structural Activity and Evolution Since the Late Quarternary on Anninghe Faults, Earthquake in Sichuan, No.4 1-12
- Wang Z., Xu, Z.,Yang,T., Hao, M., 1996, Study of diformation mechanismof the Xianshuihe river fault zone -a shallow level, high temperature ductile shear zone, Regional Geology of China , No.3, 245-251
- Xu, X., Zhang, P., Wen, X., et al, 2005, Features of active tectonics and recurrence behaviors of strong earthquakes in the western Sichuan province and its adjacent regions, Seismology and Geology, V.27, No.3, 446-461
- profile from Yanggao to Rongcheng: application of decomposition of MT tensor impedance, Seismology and Geology, V.18, no.1, 66-74

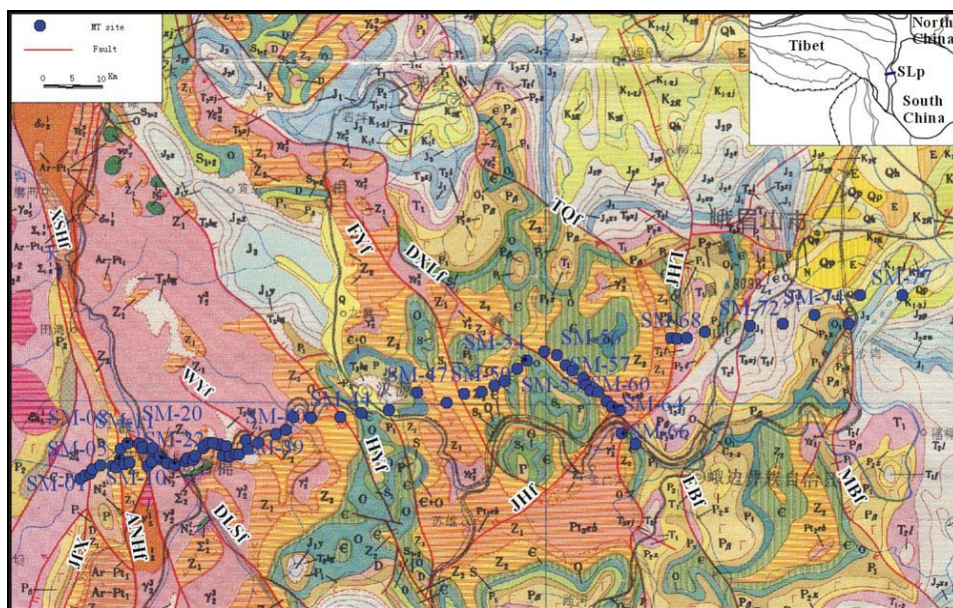


Fig.1 MT profile SLp and geologic setting. Words including suffix ‘f’ indicate the names of the faults. The south china block contains CSb, Tibet block contain CDb shown in right top picture..

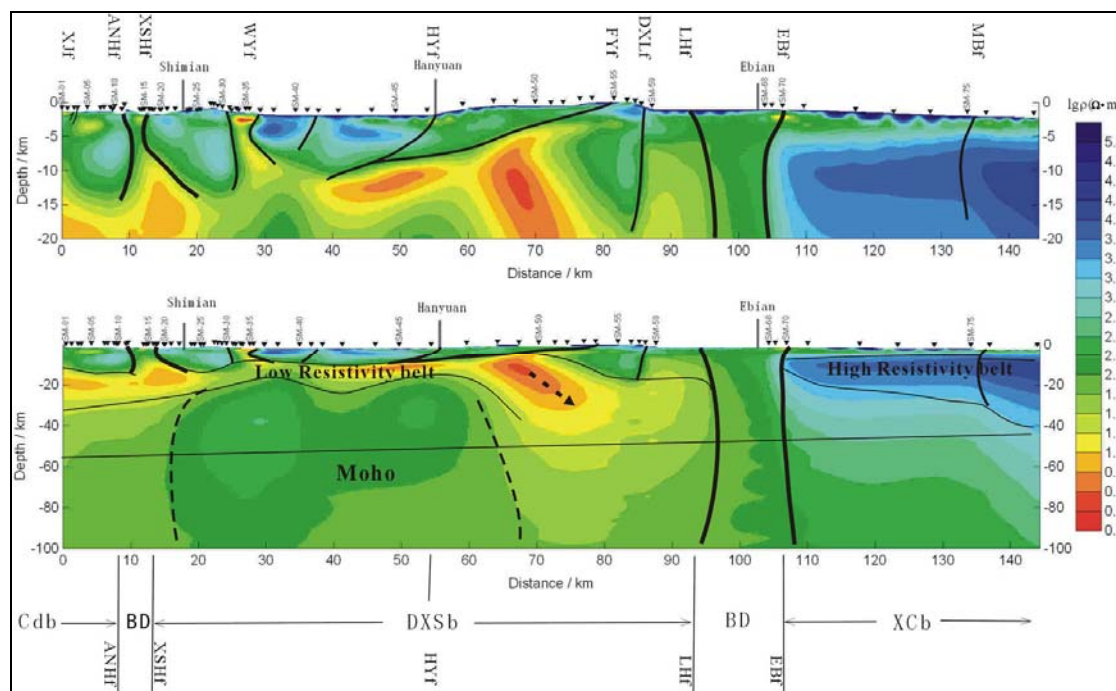


Fig.4. 2-D electrical structure and the geologic interpretation along the profile. The top and bottom show structures for 0~20 and 0~100 km respectively. reverse triangle indicates the MT sites on the surface of each profile. The fault names are corresponding to the names in the picture of fig.1. BD—boundary belt.